01 Jan 1990

Use of Energy in Data-Track Association and State Estimation in Multitarget-Multisensor Problems

S. N. Balakrishnan
Missouri University of Science and Technology, bala@mst.edu

H. Park

Recommended Citation

S. N. Balakrishnan and H. Park, "Use of Energy in Data-Track Association and State Estimation in Multitarget-Multisensor Problems," *Proceedings of the IEEE 1990 National Aerospace and Electronics Conference (1990, Dayton, OH)*, Institute of Electrical and Electronics Engineers (IEEE), Jan 1990.
The definitive version is available at https://doi.org/10.1109/NAECON.1990.112800

USE OF ENERGY IN DATA-TRACK ASSOCIATION AND STATE ESTIMATION IN MULTITARGET-MULTISENSOR PROBLEMS

S. N. Balakrishnan and Hyungwug Park

University of Missouri-Rolla
Rolla, Missouri 65401

ABSTRACT

A 'coarse' test and a 'fine test' have been formulated for use in multiple sensor-multiple target data-track association. Various forms of energies are used in these tests to pick the proper data to be associated with any target. Numerical experiments are presented through the use of a decentralized Kalman filter scheme.

I. BACKGROUND

Introduction

The advent of microprocessor based guidance and control systems and the advances in weapons technology have generated a lot of interest in analytical research in the area of multiple target-multiple sensor problems. Some of the wide-ranging applications which fall under this class of problems include ballistic missile defense, ocean surveillance of ships and submarines, tactical air defense against aircraft, warfare involving ground vehicles and military units, Geo Positioning Satellites (GPS) systems, and air traffic control.

The foremost difficulty in solving the multitarget-multisensor problem is the data discrimination associated with track correlation. If the data are not discriminated properly, it will lead to degraded tracking accuracies and divergence.

One source of difficulty is when a sensor operates in an environment in which there is clutter, or a high false-alarm rate. It can also happen when several targets are in the same neighborhood and one can not associate with certainty the observed detections, which yield the measurements, with the various targets. A similar situation can occur in the target tracking problem when there can be several targets but the number may not be known and some of the measurements may be spurious, and some targets may be thrusting suddenly. The latter scenario can occur with uncooperative targets.

The track correlation procedures in many existing systems use a nearest neighbor filter in some sense to predict the measurements. The nearest neighbor filter estimates the next position where the next data can be with a priori information and then identifies the nearest data from the estimates with the proper data for track correlation. Such methods may fail in tracking correlation especially when the target is maneuvering.

Consequently, two new tests have been devised in this study to arrive at better correlations in the presence of multiple targets. They are:

Coarse Test

(a) Potential Energy (using $\bar{x}$, where $\bar{x}$ represents the predicted mean states of targets).

(b) Positions (using $\bar{x}$)

(c) Total Energy (using $\bar{x}$)

Fine Test

(a) Total Energy (using x, where x represents the a posteriori mean states of targets).

In most of the existing literature[1,13,14,16,17,24] the measurements have been assumed to be linear components of the position states which lead to good results but untenable practical applications. An important feature in this study is the use of non-linear measurements such as range, range rate, and the bearing angle.

Methods in Literature

Single (multiple) sensor - single (multiple) target track correlation is a classical problem which has interested researchers for many years. Nine different methods have been identified in the existing literature.

(1) Nearest neighbor filter[1],
(2) Tracking via data association[2],
(3) Track-split filter[3,4],
(4) Maximum likelihood method[5,6],
(5) Probabilistic Data Association Filter[7-9,10,11],
(6) Optimal Bayes Approach[12],
(7) Joint Probabilistic Data Association Filter[13,14],
(8) Track Data Correlation Filter[5,15-17],
(9) Pattern Recognition Approach[18].

However, difficulties have been encountered in track correlation when applied to maneuvering targets. The application of improper data to track correlation could result in severely degraded tracking accuracies since typical tracking filters such as the Kalman filter do not account for such correlation error. The history of track correlation is discussed at length by Bar-Shalom[1] and Chaudhuri[19].

The method developed in this study uses the energy equations such that the track can be correlated more accurately even in the cases of maneuvering targets. The energy correlation method used in this study involves comparing the energy of the objects calculated by using the filter with the energy calculated by using the data directly. Since the kinetic energy is part of the total energy, unlike other methods, the energy correlation method is expected to distinguish between targets at the same locations and travelling with different velocities.

CH2881-1/90/0000-0375 $1.00 © 1990 IEEE

The models of the dynamic systems and the filters are described in Section II. The measurement system is also presented. The differences in using the nonlinear measurements and linear measurements are explained. In Section III, two different tests with the energy-correlation method are described. These methods are applied to various types of flying objects which are either maneuvering or non-maneuvering in Section IV. The numerical results from various tests and their interpretations are presented. Conclusions are summarized in Section V.

II. SYSTEM AND MEASUREMENT MODELS

The mathematical models of the dynamic systems and the measurements are presented in this section. The system considered in this study consists of a number of targets and sensors. Each of the targets is viewed from different sensors. A decentralized filter system is used in this study. Speyer[20] formulated this filter in the context of a decentralized linear control problem. In this study, however, there is no active control. The control part is, therefore, substituted with the acceleration due to gravity in the case of passive targets or discrete levels of acceleration in order to represent the maneuvering targets. The discrete equations describing the motion of the objects under study are given by

$$x_{i+1} = A\, x_i + B\, U_i \tag{1}$$

where x_i is the state of the target at stage i, U_i represents the accelerations experienced by the target, and A and B are known constant matrices. The four-element state vector consists of two position components and two velocity components in a two-dimensional inertial frame. In the filter, however, the target dynamics are modelled as

$$x_{i+1} = A\, x_i + B\, U_i + w_i \tag{2}$$

where w_i is a white noise sequence which has been added to account for the uncertainty in modelling. Measurements at each node (sensor) are modeled as

$$z_{ij} = H_i x_{ij} + v_{ij} \quad \text{(Linear Measurements)} \tag{3}$$

and

$$z_{ij} = h_{ij}(x_{ij}) + v_{ij} \tag{4}$$

(Nonlinear Measurements)

where z_{ij} is a measurement vector at node j at stage i, H^j is a known matrix, h_{ij} is a known vector, v_{ij} is a Gaussian noise with zero mean and known variance V_{ij}.

The best a posteriori estimate of the state of a target at stage i is assumed to be given by its conditional mean $\hat{x}_i$, as $\hat{x}_i = E[x_i | z_{i1}, \ldots z_{ik}]$, where E[a/b] represents the conditional expectation of a given b. This expression for the estimate in terms of the innovations is

$$\hat{x}_i = \bar{x}_i + \sum_{j=1}^{k} K_{ij}\, (z_{ij} - H^j \bar{x}_{ij}) \tag{5}$$

for linear measurements and

$$\hat{x}_i = \bar{x}_i + \sum_{j=1}^{k} K_{ij}\, (z_{ij} - h_{ij}\, (x_{ij})\big|_{x_{ij} = \bar{x}_{ij}}) \tag{6}$$

for nonlinear measurements.

The term, $\bar{x}_i$, in Eqs. (5) and (6) is a priori mean of x_i conditioned on measurements up to the i-1. The Kalman gain, K_{ij}, is given as $K_{ij} = P_{ij}(H_{ij})^T (V_{ij})^{-1}$, where P_{ij}, the a posteriori error variance, is given by

$$(P^j_{i+1})^{-1} = (M^j_{i+1})^{-1} + \sum_{j=1}^{k} (H_{i+1j})^T\, (V^j_{i+1})^{-1}\, (H_{i+1j}) \tag{7}$$

The a priori state error covariance, M^j_{i+1}, is propagated between the measurements as $M^j_{i+1} = AP_{ij}A^T + W_i$. In order to simplify the formulation, x_i is defined as the sum of two terms $\hat{x}_{i+1D}$ and x_{i+1C}. The term X_{iC} is due to acceleration or control and is propagated as

$$x_{i+1C} = Ax_{ic} + BU_i; \quad (x_{1C} = \bar{x}_1) \tag{8}$$

and x_{iD}, due to new data, is updated as

$$\hat{x}_{i+1D} = \bar{x}_{i+1D} + \sum_{j=1}^{k} (\bar{z}_{i+1j} - H^j \bar{x}_{i+1Dj}) :$$

$$\bar{x}_{i+1Dj} = A\hat{x}_i^{Dj} \tag{9}$$

when the measurement function is linear

$$\bar{z}_{i+1j} = z_{i+1j} - H^j x_{i+1C} \tag{10}$$

and

$$\hat{x}_{i+1D} = \bar{x}_{i+1D} + \sum_{j=1}^{k} (\bar{z}_{i+1j} - h_{i+1j}\, (\bar{x}_{i+1Dj})) :$$

$$\bar{x}_{i+1Dj} = A\hat{x}_i^{Dj} \tag{11}$$

when the measurement function is nonlinear. Note that the measurement partial derivative matrix H_{ij} is constant only if measurement function is linear. Otherwise, it is a function of the states evaluated at $x_i = \bar{x}_i$.

The decentralized system is assumed to have a local Kalman filter processing the data at each sensor. Let x_i^{Dj} be the estimate and P_{ij} be the error variance at node j of the state using only Z_{ij}. The state estimator at each node corresponding to the data is

$$\hat{x}_{iDj} = \bar{x}_{iDj} + P_i(H^j)^T (V_{ij})^{-1}\, [\bar{z}_{ij} - H^j \bar{x}_{iDj}] :$$

$$\bar{x}_{iDj} = A\hat{x}_{i-1}^{Dj} \tag{12}$$

when the measurement function is linear and

$$\hat{x}_{iDj} = \bar{x}_{iDj} + P_{ij}(H_i^j)^T (V_{ij})^{-1}\, [\bar{z}_{ij} - h_{ij}(\bar{x}_{iDj})] :$$

$$\bar{x}_{iDj} = A\hat{x}_{i-1}^{Dj} \tag{13}$$

when the measurement function is nonlinear.

The estimates from all the nodes can be combined to form the overall estimate of the state given all data as

$$x_{iC} = Ax_{iC} + BU \; : \; x_{1C} = \bar{x}_1, \; \underline{x}_1^D = 0 \qquad (14)$$

and

$$\hat{x}_{iD} = \sum_{j=1}^{k} [P_i \, (P_{ij})^{-1} \, \underline{x}_i^{Dj} + h_{ij}] \qquad (15)$$

where h_{ij} is an additional data dependent n-vector which is calculated at each node as

$$h_{i+1}^j = F_{i+1} h_{ij} + G_{i+1}^j \underline{x}_{i+1}^{Dj}, \; h_{1j} = 0. \qquad (16)$$

The terms, F_{i+1} and G_{i+1}, are

$$F_{i+1} = P_{i+1} M_{i+1}^{-1} A \qquad (17)$$

and

$$G_{i+1}^j = P_{i+1} M_{i+1}^{-1} A P_i (P_{ij})^{-1} A^{-1} - P_{i+1} (M_{i+1}^j)^{-1} \qquad (18)$$

assuming A to be nonsingular.

III. CORRELATION TECHNIQUES

Two tests are devised in this study for proper data-target association. They are termed as coarse test and fine test and described in this section at length.

Coarse Test

The coarse test is used to eliminate the more obvious non-associated sensor reports with a relatively simple test. The objective of this test is to minimize the overall computational requirements by limiting the amount of reports that must be processed through the fine test, which is more rigorous and computation intensive. A functional flow diagram for the coarse and fine tests is outlined in Figure 1.

When the targets are not maneuvering, there are no changes in the energy of targets. Thus, the difference between energy calculated through the filter and that calculated from the data should be close to zero, if the estimation process is good.

Three types of coarse tests are employed in this study. They are as follows:

(a) Potential Energy Test

In this test, the potential energy calculated from the data that has the closest number to that calculated through a priori estimates and the corresponding data are used for updating the target tracks. The potential energy using a priori estimate is given by

$$E_{P1} = G \times \bar{y} \qquad (19)$$

where $\bar{y}$ is the a priori estimate of altitude and G is the gravitational constant.

The potential energy correlated by using the observational data is given by

$$E_{P2} = G \times R \times \sin\theta \qquad (20)$$

where R is range and θ is angle as shown in Figure 2.

The data which results in the potential energy (E_{P2}) closest to the estimated potential energy (E_{P1}) is associated with the track for updating the post-eriori state estimates. Note that the potential energy test becomes useless if there are two or more targets at the same altitude.

(b) x-Position Test

The objective of the x-position test is similar to the potential energy test. The x-position of the targets from the filter and the data are compared. This is performed with an inequality given by

$$\bar{x}_i - \alpha < R \cos\theta < \bar{x}_i + \alpha \qquad (21)$$

where $R \cos\theta$ is the x position of data, $\bar{x}_i$ is the x position of a priori estimate and the maximum difference between x position of a priori estimate and x position of data is α.

$$\alpha = \frac{1}{2} \times \text{Maximum acceleration} \times (\text{Time interval})^2 + \sqrt{\text{Computed position error variance}}$$

(c) Total Energy

If the targets are not maneuvering, proper data may be identifiable with the track through the total energy test because total energies include velocities. If the targets are maneuvering, then this test has a likelihood of failure. The total energy using a priori estimate is given by

$$E_1 = \frac{1}{2} (\bar{x}^2 + \bar{y}^2) + G \, \bar{y} \qquad (22)$$

and the total energy using data is given by

$$E_2 = \frac{1}{2} (\dot{R}^2 + \bar{R}\dot{\theta}^2) + G \, R \sin\theta \qquad (23)$$

where $\dot{R}$ is a range-rate and $\bar{\theta}$ is calculated from data and the a priori state estimates as

$$\bar{\theta} = \frac{R \cos\theta \bar{y} - R \sin\theta \bar{x}}{R^2} \qquad (24)$$

The total energy (E_2) is bounded by the inequality

$$E_1(1 - \beta) < E_2 < E_1 \, (1 + \beta) \qquad (25)$$

where β reflects maximum energy change rate with respect to thrusting case.

If E_2 does not satisfy the limit, the process goes back to the beginning, Figure 1. This inequality is set to pick out the proper data by setting a limit total energy in the data which passed the potential energy test and the x position test.

Fine Test

(a) Total Energy

In this method, the updated estimates of the position and the velocity are obtained from the data

selected through the coarse test. Then, they are used to compute the total energy, E_3, and compare it with E_2 (energy using data). That is,

$$E_2 = \frac{1}{2}(\dot{R}^2 + \hat{R\theta}^2) + G\,R\,\sin\theta \qquad (26)$$

where θ is calculated from data and the a posteriori estimates as

$$\hat{\theta} = \frac{R\cos\theta\hat{y} - R\sin\theta\hat{x}}{R^2} \qquad (27)$$

and

$$E_3 = \frac{1}{2}(\hat{x}^2 + \hat{y}^2) + G\hat{y} \qquad (28)$$

The energy is again bounded by

$$E_3(1 - \gamma) < E_2 < E_3\,(1 + \gamma) \qquad (29)$$

where γ which reflects maximum energy change rate is less than β.

If E_2 does not satisfy the limit, the process shifts back to first step in Figure 1. This test is especially useful if the targets are thrusting. In such an event, the velocities, and therefore, the total energy will change. Since the filter model cannot pick up the acceleration due to thrust at once, there may be a large difference in E_1 (energy using a priori estimates) and E_2 (energy using data). However, since thrusting is accounted for in E_3 (energy using posteriori estimates), E_2 and E_3 are almost the same. Hence, larger numerical values will be assumed for β than for γ.

IV. NUMERICAL RESULTS

In order to measure the usefulness of the energy tests, three different scenarios have been simulated.

The first case consists of two flying objects with a flight time of 5 seconds. This simple case demonstrates the use of the energy in proper correlation of data with tracks. The second test case is more complex with ten objects with a flight time of about 5 seconds. The third numerical experiment consists of two long range rockets with a range of about 7000 kms.

In all these cases, the elements of the state space consist of two components of positions and two components of velocities in an inertial cartesian frame. The number of sensors is two.

The measurement sets consist of 1) relative position components from sensors to object, 2) relative range and bearing angle from sensors to objects, (3) relative range, relative range rate, and bearing angle.

The numerical values of the parameters used in the simulation are presented in Table I. Trajectories of the two objects and the maneuvering long range rockets are presented in Figures 3 and 4.

Five tables consisting of the values of the different energy levels are presented to illustrate the efficacy of energy as a good data-track correlator.

The energy levels of a two-object scenario is presented in Table II. When the altitude and the x-component of position of the targets are spaced enough to identify the proper data, proper correlation is accomplished by comparing the potential energy and the x-position used in coarse tests. For example, the difference between E_1 and E_2 between the objects 1 and 2 is almost 15 in as can be seen from Table II.

When the altitude and the x-component of the position are close, but not the velocities, the third part of the coarse test with the help of total energy helps in proper data-track association. It can be observed from Table III that the differences between the potential energy or x-position of the two objects are small. However, the kinetic energies are different enough so that the total energy of object 1 is almost twice that of object 2 and this feature has helped in proper data association. Note that in these two cases, a wrong association of data leads to very different energy levels.

A representative case from the scenario with 10 flying objects is presented in Table IV. The usefulness of the energy tests can be easily observed. When the objects are maneuvering, the apriori estimates are quite different from posteriori estimates. The effectiveness of the fine test with the posteriori estimates is brought out in Table V.

A typical time instant in the long-range rocket trajectory is used in Table VI to illustrate the effectiveness of the energy tests in yet another different type of scenario.

Representative estimation histories of positions for the case of two objects and the long-range rockets are presented in Figures 5 - 8. Note that with proper association of sensor reports, the trajectories can be tracked with accuracies varying only with measurement accuracies.

V. CONCLUSIONS

Two types of tests have been devised for data-track correlation in a multiple sensor - multiple object environment. These tests use various kinematic parameters of the object to compute different forms of energy by using the filter parameters and data. Numerical experiments show the effectiveness of these tests.

REFERENCES

1. Bar-Shalom, Y., "Tracking Methods in a Multitarget Environment," IEEE Trans. on Automatic Control, Vol. AC-23, No. 4, August 1978.

2. R. W. Sittler, "An Optimal Data Association Problem in Surveillance Theory," IEEE Trans. Mil. Elec., Vol. MIL-8, pp. 125-139, April 1964.

3. E. C. Fraser and L. Meier, "Mathematical Models and Optimum Computation for Computer-Aided Active Sonar System," U.S. Navy Electronic Lab., SRI Final Rept. (First Year), San Diego, CA, Contract N123-(953)54486A, March 1967.

4. P. Smith and G. Buechler, "A Branching Algorithm for Discriminating and Tracking Multiple Objects," IEEE Trans. Automatic Control, Vol. AC-20, pp. 101-104, February 1975.

5. Stein, J. J. and Blackman, S. S., "Generalized Correlation of Multitarget Track Data," IEEE Trans. Aerospace and Electronics Systems, AES-11, No. 6, pp. 1207-1217, November 1975.

6. C. L. Morefield, "Application of 0-1 Integer Programming to Multitarget Tracking Problems," in Proc. IEEE Conf. Decision and Control, Dec. 1975 and IEEE Trans. Automat. Contr., Vol. AC-22, pp. 302-312, June 1977.

7. R. G. Sea, "An Efficient Suboptimal Decision Procedure for Associating Sensor Data with Stored Tracks in Real-Time Surveillance Systems," in Proc. IEEE Conf. on Decision and Control, pp. 33-37, Miami Beach, FL, Dec. 1971.

8. R. A. Singer and J. J. Stein, "An Optimal Tracking Filter for Proc. Sensor Data of Imprecisely Determined Origin in Surveillance Systems," in Proc. IEEE Conf. Decision and Control, pp. 171-175, Miami Beach, FL, Dec. 1971.

9. R. A. Singer and R. G. Sea, "New Results in Optimizing Surveillance System Tracking and Data Correlation Performance in Defense Multitarget Environments," IEEE Trans. Automat. Contr., Vol. AC-18, pp. 571-581, Dec. 1973.

10. Y. Bar-Shalom and A. Jaffer, "Adaptive Nonlinear Filtering for Tracking with Measurements of Uncertain Origin," IEEE Conf. Decision and Control, pp. 243-247, New Orleans, LA, Dec. 1972.

11. Y. Bar-Shalom and E. Tse, "Tracking in a Cluttered Environment with Probabilistic Data Association," in Proc. 4th Symp. Nonlinear Estimation, Univ. California, San Diego, Sept. 1973, and Automatica, Vol. 11, pp. 451-460, Sept. 1975.

12. R. A. Singer, R. G. Sea, and K. Housewright, "Derivation and Evaluation of Improved Tracking Filters for Use in Dense Multitarget Environments," IEEE Trans. Inform. Theory, Vol. IT-20, pp. 423-432, July 1974.

13. T. Fortman, Y. Bar-Shalom, and M. Scheffe, "Multitarget Tracking Using Probabilistic Data Association," Proceedings 19th IEEE Conf. Decision and Control, Albuquerque, NM, December 1980, and IEEE J. Ocean Engr., July 1983.

14. D. B. Reid, "An Algorithm for Tracking Multiple Targets," IEEE Trans. Automatic Control, AC-24, 843, 1979.

15. Bowman, "Maximum Likelihood Track Correlation for Multisensor Integration," IEEE Decision and Control Conf., 1979.

16. Chang, C. B. and Youens, L. C., "An Algorithm for Multiple Target Tracking and Data Correlation," Technical Report TR-643, Lincoln Lab, M.I.T., 13 June 1983.

17. Singer, R. A. and Kanyuck, A. J., "Computer Control of Multiple Site Track Correlation," Automatica, Vol. 7, pp. 455-464, July 1971.

18. S. P. Chaudhuri, "A General Approach to the Development of Passive/Active Sensor Data Fusion," American Control Conference, pp. 823-828, June 1985.

19. Balakrishnan, S. N. and Tapley, B. D., "Multitarget Classification and Estimation Using Clustering Techniques," AIAA Journal of Guidance, Control, and Dynamics, Vol. 13, No. 1, Jan.-Feb. 1990, pp. 121-127.

20. J. L. Speyer, "Computation and Transmission Requirements for a Decentralized Linear-Quadratic-Gaussian Control Problem," IEEE Trans. on Automatic Control, Vol. AC-24, pp. 266-269, April 1979.

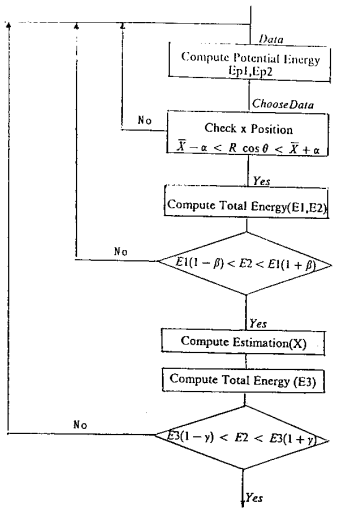

Figure 1. Functional Flow Diagram.

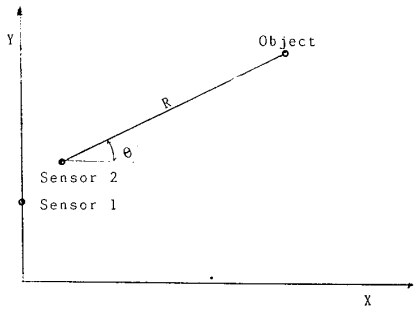

Figure 2. Measurements in Inertial Frame.

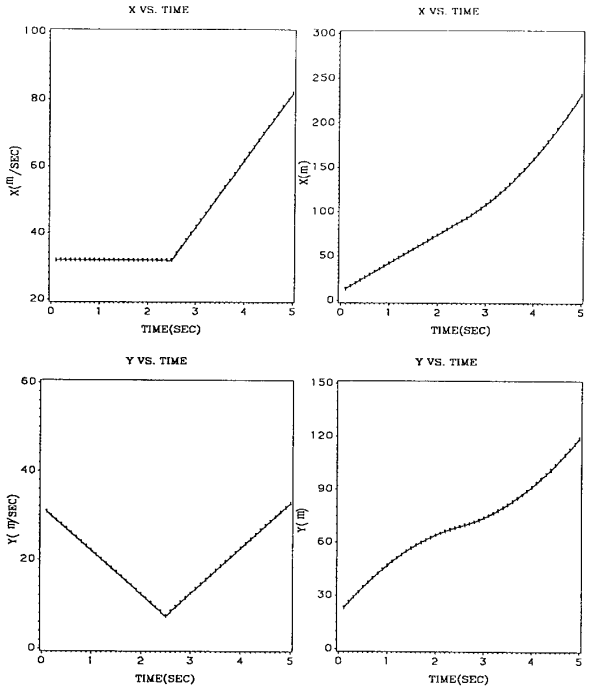

Figure 3. Trajectories of Two Objects.

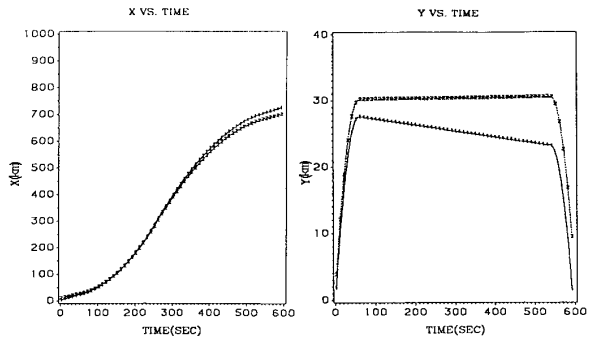

Figure 4. Trajectories of Two Long Range Rockets.

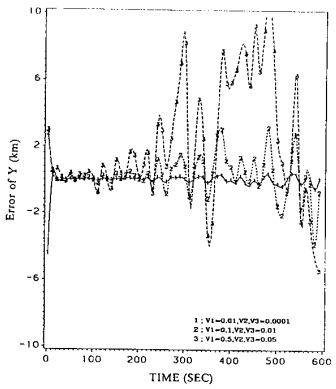

Figure 8. Error History of y-Position (Long Range Rocket).

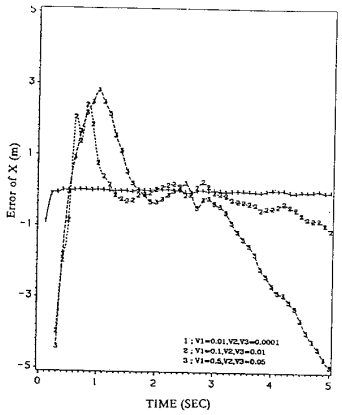

Figure 5. Error History of x-Position.

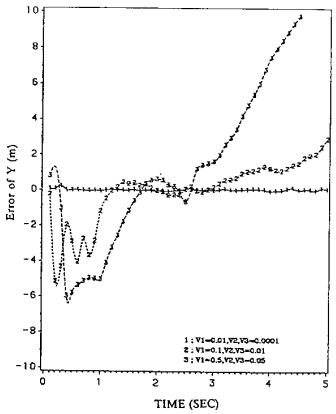

Figure 6. Error History of y-position.

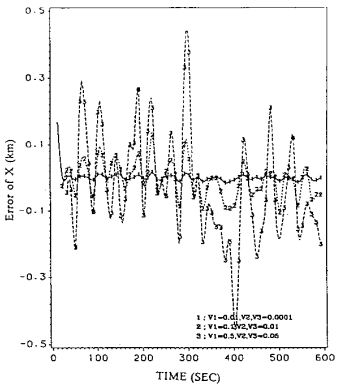

Figure 7. Error History of x-Position (Long Range Rocket).

Table I. Values of Parameters.

CASE	P	w1	w2	V1	V2	V3	Time interval
a	100	0.01	4.	0.01 0.1 0.5	0.0001 0.01 0.05	0.0001 0.01 0.05	0.1
b	100	0.01	4.	0.01 0.1 0.5	0.0001 0.01 0.05	0.0001 0.01 0.05	0.1
c	100	0.005	0.005	0.01 0.1 0.5	0.0001 0.01 0.05	0.0001 0.01 0.05	2.0

a = Two-flying-objects case

b = Ten-flying-objects case

c = Intermediate range ballistic missile

P = Initial error variance

w1 = State noise of the position

w2 = State noise of the velocity

V1 = Gaussian noise of the range

V2 = Gaussian noise of the angle

V3 = Gaussian noise of the range-rate

Table II. Energy Levels - Two Object Scenario.

Time	Object	E1	E2	X1	X2	E3	E4	E5	E6
2.2	1	543.73	552.36	104.91	104.87	1633.60	1630.18	1633.39	1443.19
	2	574.34	571.95	106.91	106.87	1652.94	1649.42	1702.12	1462.05
2.4	1	589.66	588.33	113.47	113.54	1635.12	1763.57	1754.97	1457.69
	2	602.26	607.92	115.47	115.47	1655.07	1783.66	1813.55	1492.24

Where E1 = Potential energy using $\bar{X}$ E2 = Potential energy using data

E3 = Total energy using $\bar{X}$ E4 = Total energy using data

E5 = Total energy using $\dot{X}$ with proper data E6 = Total energy using $\dot{X}$ with improper data

X1 = X position of $\bar{X}$ X2 = X position of data.

Table III. Energy Levels - Two Object Scenario (Total Energy Test).

Time	Object	E1	E2	X1	X2	E3	E4	E5
1.6	1	209.87	210.93	54.05	53.91	850.03	849.12	449.72
	2	210.16	211.26	54.08	53.94	449.41	448.41	851.34

Where E1 = Potential energy using $\bar{X}$ E2 = Potential energy using data

E3 = Total energy using $\bar{X}$ E4 = Total energy using proper data

E5 = Total energy using improper data X1 = X position of $\bar{X}$

X2 = X position of data.

Table IV. Energy Levels (Ten Objects).

Time	Object	E1	E2	X1	X2	E3	E4	E5	E6
1.6	1	352.834	366.178	58.076	57.409	1013.972	1029.753	1014.012	1022.405
	2	397.997	412.257	57.898	57.055	909.533	927.723	905.967	911.642
	3	380.998	396.006	70.954	70.290	1660.164	1673.863	1675.171	1679.368
	4	441.828	454.116	55.033	54.203	1620.437	1630.668	1633.738	1636.344
	5	341.265	352.559	48.345	47.708	1091.228	1100.767	1103.181	1105.471
	6	420.678	433.094	54.721	53.924	1372.687	1383.524	1385.329	1388.360
	7	191.182	204.237	60.576	60.311	1070.562	1081.459	1081.610	1086.515
	8	301.796	313.951	53.478	52.944	1091.035	1101.514	1103.452	1106.852
	9	588.487	606.289	92.283	91.281	3058.813	3074.976	3070.557	3077.650
	10	327.709	336.982	37.826	37.201	1043.348	1050.481	1053.950	1056.395

Where E1 = Potential energy using $\bar{X}$ E2 = Potential energy using data

E3 = Total energy using $\bar{X}$ E4 = Total energy using data ($\hat{\theta}$ using $\bar{X}$)

E5 = Total energy using $\dot{X}$ with proper data E6 = Total energy using data ($\hat{\theta}$ using $\dot{X}$)

X1 = X position of $\bar{X}$ X2 = X position of data.

Table V. Energy Levels (Maneuvering Objects).

Time	Object	E1	E2	X1	X2	E3	E4	E5	E6
2.6	1	475.834	476.341	93.403	93.405	1034.164	1120.652	1074.739	1062.887
	2	484.062	484.748	89.232	89.223	926.735	1000.199	938.318	922.410
	3	617.852	616.450	118.16	118.08	1681.597	1805.186	1791.057	1775.234
	4	752.160	751.557	93.488	93.394	1639.619	1758.940	1760.045	1745.831
	5	563.131	563.780	80.351	80.345	1110.417	1204.321	1204.333	1192.696
	6	686.925	686.745	89.952	89.895	1392.461	1498.764	1498.892	1485.377
	7	316.185	316.611	103.06	103.07	1091.726	1191.036	1173.476	1160.988
	8	494.457	495.015	89.257	89.258	1111.284	1208.122	1193.004	1178.839
	9	977.827	972.842	154.99	155.36	3079.172	3253.371	3268.260	3241.657
	10	575.237	576.202	65.835	65.795	1056.818	1150.287	1147.125	1137.867

Where E1 = Potential energy using $\bar{X}$ E2 = Potential energy using data

E3 = Total energy using $\bar{X}$ E4 = Total energy using data ($\hat{\theta}$ using $\bar{X}$)

E5 = Total energy using $\dot{X}$ with proper data E6 = Total energy using data ($\hat{\theta}$ using $\dot{X}$)

X1 = X position of $\bar{X}$ X2 = X position of data.

Table VI. Energy Levels (Long Range Rockets)

Time	Object	E1	E2	X1	X2	E3	E4	E5	E6
72.	1	0.076	0.079	37.755	37.645	0.254	0.267	0.258	0.267
	2	0.104	0.107	40.394	40.305	0.251	0.263	0.254	0.263
402.	1	0.064	0.013	588.724	588.763	0.985	0.937	0.958	0.935
	2	0.123	0.073	574.077	574.061	0.974	0.928	0.948	0.925
542.	1	0.013	0.062	706.857	706.879	0.115	0.162	0.131	0.156
	2	0.088	0.134	684.756	684.841	0.166	0.211	0.182	0.206

Where E1 = Potential energy using $\bar{X}$ E2 = Potential energy using data

E3 = Total energy using $\bar{X}$ E4 = Total energy using data ($\hat{\theta}$ using $\bar{X}$)

E5 = Total energy using $\dot{X}$ with proper data E6 = Total energy using data ($\hat{\theta}$ using $\dot{X}$)

X1 = X position of $\bar{X}$ X2 = X position of data.